Dissociative Photoionization of Methoxycarbonylsulfenyl Chloride, $CH_3OC(O)SCl$, Following Sulfur 2p, Chlorine 2p, and Oxygen 1s Excitations†

Mauricio F. Erben,‡ Mariana Geronés,‡ Rosana M. Romano,‡ and Carlos O. Della Védova*,‡,§

CEQUINOR (CONICET-UNLP), Departamento de Química, Facultad de Ciencias Exactas. Universidad Nacional de La Plata, C. C. 962 (1900) La Plata, República Argentina, and Laboratorio de Servicios a la Industria y al Sistema Científico (LaSeISiC) (UNLP-CIC-CONICET), Camino Centenario e/505 y 508, (1903) Gonnet, República Argentina

Received: February 5, 2007; In Final Form: May 30, 2007

Total ion yield spectra and photoinduced fragmentations following S 2p, Cl 2p, and O 1s inner shell excitations of methoxycarbonylsulfenyl chloride, $CH_3OC(O)SCl$, have been studied in the gaseous phase by using synchrotron radiation and multicoincidence techniques, which include photoelectron−photoion coincidence (PEPICO) and photoelectron−photoion−photoion coincidence (PEPIPICO) time-of-flight (TOF) mass spectrometry. According to the analysis of the partial ion yield spectra the S^+ ion signal shows a steep enhancement near the S 2p resonance, which could represent an evidence of state-specific fragmentations promoted by electronic excitations from the S 2p to vacant orbitals with strong antibonding character mainly located at the sulfur atom. The dissociation dynamics for selected PEPIPICO islands have been discussed. Fragmentation channels that involve the extrusion of H^+ and CH_x^+ ($x = 0, 1, 2, 3$) fragments have been predominantly observed for dissociation of doubly charged $CH_3OC(O)SCl^{2+}$.

Introduction

In recent years, the study of the dissociation dynamics of isolated molecules excited with energies in the vacuum ultraviolet (VUV) and soft X-ray regions has shown important advances, primarily because of the availability of synchrotron radiation sources together with the use of coincidence techniques as tools for the detection of charged particles. The main products of photodissociation processes in these energy regions are positive ions, which can be conveniently detected by means of time-of-flight (TOF) spectrometric based methods.[1] Moreover, multicoincidence spectroscopies are well-known techniques which make possible the measurement of the arrival times of each charged particle at a detector in a correlated manner.[2,3]

In contrast to valence electrons, which can be formally considered as occupying localized or delocalized molecular orbitals over the whole molecule, core- and shallow-shell electrons are highly localized on a specific atomic level of a molecule. Thus, differences in relative yields of fragment ions were observed in simple molecules by exciting *K* shell electrons.[4,5] The tunable synchrotron radiation can selectively excite inner shell electrons. If the dissociation occurs before the electronic rearrangement site- and element-specific fragmentations can be anticipated.[4,6−9]

The radiation can initiate electronic changes in the molecules, which can rearrange in a few femtoseconds. This process is considered to be practically "instantaneous" for all chemical purposes (Franck−Condon principle). The insight into the nature of the site specific fragmentation is of importance in understanding localization phenomena in chemical reactions.[10] Moreover, photoinduced processes at solid surfaces have attracted much attention not only as a fundamental science but also as technological applications, because they provide a unique route for the synthesis of new materials through non thermal reactions.[11]

Our research group has quite recently started studies concerning shallow- and inner-core electrons in sulfenylcarbonyl compounds. Total ion yield (TIY) and partial ion yield (PIY) spectra, as well as multicoincidence spectra (photoelectron-photoion coincidence, PEPICO, and photoelectron−photoion−photoion−coincidence, PEPIPICO) were measured for the S 2p, Cl 2p, C 1s, O 1s, and F 1s transitions of $FC(O)SCl$[12] and $ClC(O)SCl$[13] by using synchrotron radiation in the 100−1000 eV range. The branching ratios for ion production obtained from the PEPICO spectra for these both species exhibit only a small dependence on the incident photon energy, which was interpreted in terms of a "lose memory" effect after an Auger decay, promoted by the delocalization of valence orbitals over the entire planar molecule.[14,15] On the other hand, a similar experimental study carried out for thioacetic acid, $CH_3C(O)SH$, was interpreted in terms of a moderate site-specific fragmentation evidenced by a diminution of the CH_3CO^+ fragment signal in going from the S 2p to the O 1s transition regions.[16]

In spite of its versatility in synthetic applications, and considering molecular characterization as a central part of the chemistry, the structural and spectroscopic properties of the methoxycarbonylsulfenyl chloride molecule have been only recently reported.[17] Additionally, the reaction of H atoms with $CH_3OC(O)SCl$ at room temperature was studied by infrared chemiluminescence techniques.[18]

The main goal of the present study of $CH_3OC(O)SCl$ is to obtain evidence regarding the electronic transitions throughout the whole region of the S and Cl 2p shallow-core and O 1s core edges as well as the ionic dissociation mechanisms

† This work is part of the thesis of M.G., who is a doctoral fellow of CONICET. C.O.D.V., R.M.R. and M.F.E. are members of the Carrera del Investigador of CONICET.

* To whom correspondence should be addressed. E-mail: carlosdv@quimica.unlp.edu.ar.

‡ Universidad Nacional de La Plata.

§ LaSeISiC.

10.1021/jp0709961 CCC: $37.00
Published on Web 07/28/2007

following the electronic relaxation of the core excited $CH_3OC(O)SCl$. The methodology includes the use of multicoincidence TOF−mass spectroscopy techniques and tunable synchrotron radiation. Fragmentation patterns deduced from PEPICO spectra at various excitation energies in the VUV and soft X-ray regions were especially analyzed in order to establish the existence of a site-specific fragmentation effect. Also, ionic double coincidences were examined, and dissociation mechanisms were proposed to explain the shape and slope of observed PEPIPICO islands.

Experimental

Synchrotron radiation was used at the Laboratório Nacional de Luz Síncrotron (LNLS), Campinas, São Paulo, Brazil.[19] Linearly polarized light monochromatized either by a toroidal grating monochromator (available at the TGM beam line in the range 12−300 eV)[20] or by a spherical grating monochromator (available at the SGM beam line in the range 200−1000 eV), intersects the effusive gaseous sample inside a high vacuum chamber, with base pressure in the range 10^{-8} mbar. During the experiments the pressure was maintained below 10^{-5} mbar. At the LNLS, the TGM and SGM beamlines resolution power are better than 400 and 3000, respectively. The intensity of the emergent beam was recorded with a light-sensitive diode. The ions produced by the interaction of the gaseous sample with the light beam were detected using a time-of-flight (TOF) mass spectrometer of the Wiley-Mac Laren type for both PEPICO and PEPIPICO[21,22] measurements. This instrument was constructed at the Institute of Physics, Brasilia University, Brasilia, Brazil.[23] The axis of the TOF spectrometer was perpendicular to the photon beam and parallel to the plane of the storage ring. Electrons were accelerated to a multichannel plate (MCP) and recorded without energy analysis. This event starts the flight time determination process of the corresponding ion, which is consequently accelerated to another MCP.

The sample of methoxycarbonylsulfenyl chloride, $CH_3OC(O)SCl$, was obtained from commercial sources (Aldrich, estimated purity 97%). The liquid sample was purified by repeated trap-to-trap distillation in vacuum. The purity of the compound in both vapor and liquid phases was checked by IR and ^1H NMR spectroscopies, respectively. Highly pure samples were used in the experiments, and the presence of thermodynamic decomposition products are unlike due to the inherent thermal stability of the sample.

The core equivalent model[24,25] was implemented in order to estimate S 2p and O 1s core ionization energies, taking OCS as reference compound [experimental ionization energy of OCS (170.6 eV)].[26,27] This approximation has been shown to give a good description for carbonyl compounds.[28,29] The Cl 2p binding energy has been estimated using CH_3Cl as the reference compound (206.26 eV).[30,31] Core equivalent related calculations were performed at the UB3LYP/6-311++G** level of approximation as implemented in the Gaussian98 programs.[32]

Results and Discussion

Total Ion Yield Spectra (TIY). The TIY spectra were obtained by recording the count rates of the total ions while the photon energy is scanned. At high photon energies corresponding to shallow- and core−shell electronic levels, the quantum yield for molecular ionization is quite likely tending to unity. Consequently, the detection of parent and fragment ions as a function of the incident photon energy is a powerful method to be used as a complement to absorption spectroscopy.[33] The TIY spectrum of $CH_3OC(O)SCl$, measured near the S 2p edge is shown in Figure 1. Below the S 2p threshold, the spectrum is dominated by a group of six signals centered at 162.5, 163.3, 165.3, 166.0, 166.9, and 168.2 eV, while the ionization edge is located at approximately 171.0 eV. Two of these signals may correspond to transitions involving the spin−orbit split of the 2p term in the $2p_{1/2}$ and $2p_{3/2}$ levels in the excited species to unoccupied antibonding orbitals and in agreement with the $2J + 1$ rule, an intensity ratio of 1:2 is expected for these transitions. In the case of the simplest sulfide, H_2S, this splitting was reported to be 1.201 eV.[34] A rather complex feature is observed below the threshold, and Rydberg series corresponding to the S 2p excitations cannot be ruled out. Furthermore, the nonresonant X-ray emission spectrum for OCS at the S 2p edge shows a clear sign of breakdown of the molecular−orbital picture in this region due to high density overlapping and vibrational broadening.[27] This assignment for the $CH_3OC(O)SCl$ molecule should be taken as tentative, since an unambiguously description of the excitations appearing below the S 2p ionization potential is not likely to assess for such a large molecule by using our available techniques.

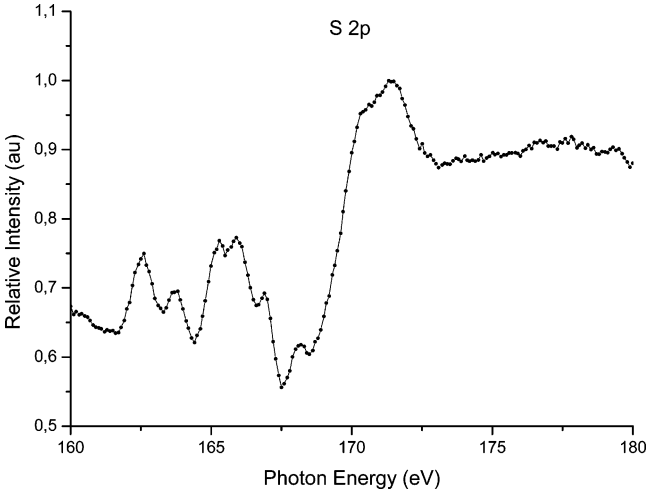

Figure 1. Total ion yield spectrum of $CH_3OC(O)SCl$ near the S 2p region.

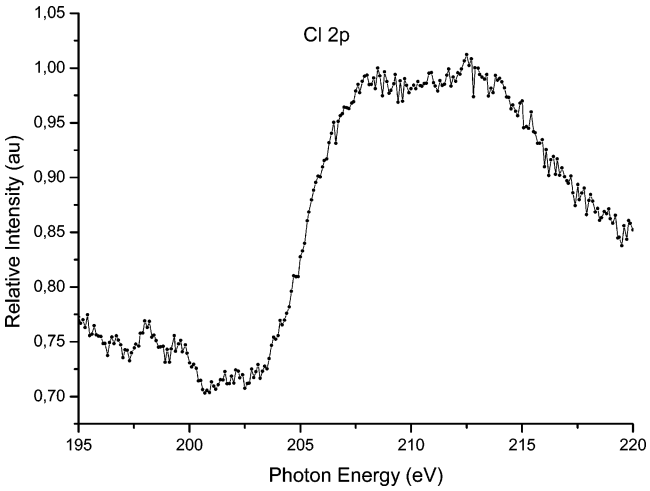

Figure 2. Total ion yield spectra of $CH_3OC(O)SCl$ in the Cl 2p region.

The TIY spectrum measured near the Cl 2p region is shown in the Figure 2. The Cl 2p threshold is located at approximately 207.0 eV and below this photon energy two signals can be observed at 198.0 and 199.3 eV. The observed resonance transitions may be mainly assigned to transitions involving the spin−orbit split of the 2p term in the $2p_{1/2}$ and $2p_{3/2}$ levels of the excited chlorine species.

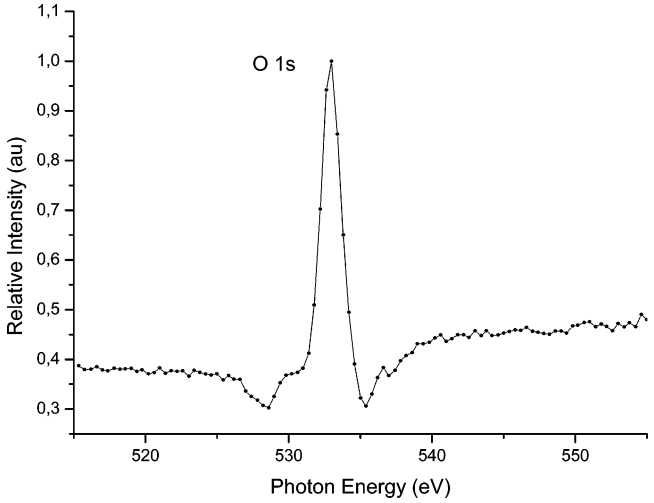

Figure 3. Total ion yield spectra of $CH_3OC(O)SCl$ in the O 1s region.

Figure 3 displays the TIY spectrum obtained near the O 1s region. This spectrum is dominated by an intense resonance centered at 533.0 eV, whereas the O 1s threshold is located at approximately 539.0 eV. A shoulder at 530.0 eV and a low-intensity signal at 536.6 eV were also observed. As has been reported for other carbonyl compounds, electronic excitations to vacant antibonding $\pi^*_{C=O}$ and $\sigma^*_{C=O}$ orbitals may be associated with the signals observed at 533.0 and 536.6 eV, respectively. However, for a complete description of the O 1s edge region in $CH_3OC(O)SCl$ transitions involving core electrons from both oxygen atoms present in the molecule should be taken into account. At the resolution used in the present experiments, it becomes apparent that the different chemical environments of the two oxygen atoms do not cause any appreciable signal shift.

The S 2p, Cl 2p, and O 1s ionization energies for $CH_3OC(O)SCl$ obtained from the TIY spectra were compared with values derived from the equivalent-core approximation. The calculated S 2p, Cl 2p, and O 1s binding energies at 170.8, 206.6, and 538.3 eV are in good agreement with the experimental values, measured at around 170.0, 207.0, and 539.0 eV, respectively.

PEPICO Spectra. Several PEPICO spectra that include the most important S 2p, Cl 2p, and O 1s transitions of $CH_3OC(O)SCl$ have been recorded. In order to identify the role of resonant Auger processes in the fragmentation, spectra were not only measured at the resonant values (maxima of the absorptions) but also at photon energy values below (typically 10 eV) and above (typically 50 eV) each resonance. For all spectra, the intensity of each ionic fragment is obtained as the integrated area under the peak, fitting as a Gaussian function to the time-of-flight spectra.

Ionic Fragmentation Near the S 2p Shallow-Core Edge. The PEPICO spectra near the S 2p edge of $CH_3OC(O)SCl$ are shown in Figure 4. In Table 1 the corresponding branching ratios are collected for the main fragment ions. The most intense peak for the resonant energy ranges under the threshold is observed for the CH_3^+ ion (14% approximately). The next most abundant ions, with relative intensities between 7 and 13%, are S^+ ($m/z = 32$), HCO^+ ($m/z = 29$), and Cl^+ ($m/z = 35$). At 171.0 eV (S 2p threshold) an increment in the intensity of the amu/q = 32 peak corresponding to the S^+ ion can be observed being the most abundant ion at this energy (16% approximately). Other less abundant ions are the following: H^+ ($m/z = 1$), SCl^+ ($m/z = 67$), the methyl fragments CH_x^+($x = 0, 1, 2,$) with $m/z = 12$, 13, and 14, O^+ or S^{2+} ($m/z = 16$), CO^+ ($m/z = 28$), CH_2O^+ ($m/z = 30$), and COS^+ ($m/z = 60$). The intensity of the signal at $m/z = 32$ amu/q, corresponding to the S^+ ion, increases when the incident photon energy is increased. An increment in the intensity of the $m/z = 35$ amu/q ion signal can be seen at 171.0 eV (S 2p threshold). Signals for the CO_2^+ ($m/z = 44$ amu/q) and $CH_3OC{=}O^+$ ($m/z = 59$ amu/q) ions also appear in these spectra, having weak relative intensity. Surprisingly, the parent ion, $CH_3OC(O)SCl^+$, can be observed as a very low intense signal in all PEPICO spectra and shows the characteristic chlorine isotopic distribution.

As discussed previously, the transitions that appear in the TIY spectra just below 171.0 eV can be interpreted as originating from the overlap of several discrete resonance

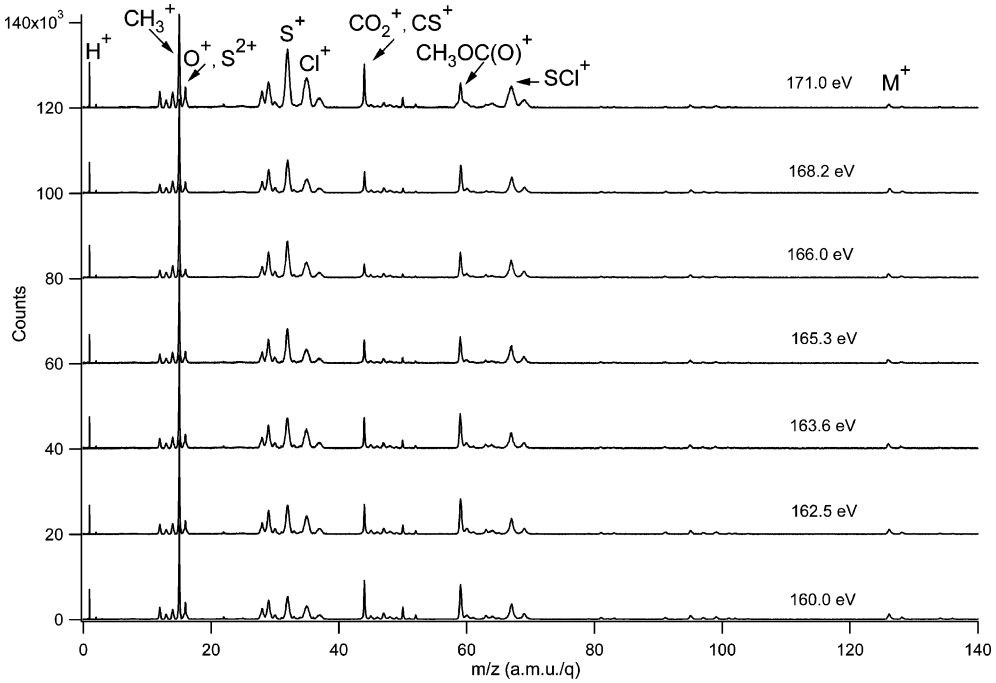

Figure 4. PEPICO spectra of $CH_3OC(O)SCl$ recorded near the S 2p edge.

TABLE 1: Branching Ratios (%) for Fragment Ions Extracted from PEPICO Spectra Taken at Photon Energies around the S 2p Energies for $CH_3OC(O)SCl$

		branching ratios at various *m/z* values (amu/q)																
electronic edge	photon energy (eV)	1 (H^+)	12 (C^+)	13 (CH^+)	14 (CH_2^+)	15 (CH_3^+)	16 (O^+/S^{2+})	17.5[a] (Cl^{2+})	28 (CO^+)	29 (HCO^+)	30 (OCS^{2+})	32 (S^+)	35[a] (Cl^+)	44 (CO_2^+)	59 ($CH_3OC{=}O^+$)	60 (OCS^+)	67[a] (SCl^+)	126[a] (M^+)
S 2p	160.0	4.0	3.0	1.7	3.1	14.1	4.6		3.5	6.5	1.9	8.7	7.1	9.1	3.5	1.6	4.9	1.0
	162.5	3.7	2.5	1.6	3.0	13.7	3.6		3.3	7.2	2.2	10.7	8.6	7.1	3.7	2.0	4.7	0.9
	163.6	3.9	2.7	1.9	3.4	13.5	4.1		3.8	6.7	2.1	10.4	7.7	3.4	5.3	1.5	4.9	1.0
	165.3	4.0	2.6	1.9	3.6	14.6	3.8		4.0	7.5	2.3	12.2	6.7	3.0	4.3	1.2	5.7	0.9
	166.0	4.2	2.3	2.1	3.7	13.7	2.9		3.7	8.0	2.5	12.8	7.1	2.3	3.8	1.4	5.6	0.9
	168.2	3.9	2.3	1.9	3.6	14.0	3.0		4.0	8.4	2.0	13.0	6.5	5.9	4.5	1.4	5.1	0.9
	171.0	3.7	2.5	1.7	3.2	11.6	3.7		3.7	6.7	1.7	16.1	10.2	7.4	3.0	1.2	5.9	0.5
Cl 2p	198.0	5.8	2.4	2.1	4.0	11.9	2.9	0.5	4.4	7.3	1.9	17.4	13.6	2.5	3.0	2.2	5.1	0.2
	208.5	5.7	2.2	2.2	3.7	11.5	2.1	0.7	6.6	8.4	1.1	23.1	5.5	4.1	4.1	1.1	7.5	0.2
	212.2	8.1	2.5	2.3	3.9	11.9	2.4	0.7	4.0	7.0	1.8	15.5	16.1	2.1	1.8	2.2	4.0	0.1
	260.0	11.0	3.3	2.7	4.1	10.0	2.9	1.0	4.1	6.2	1.5	16.1	17.1	2.1	1.4	1.7	3.1	0.1
O 1s	523.0	8.5	5.2	2.3	2.1	3.6	5.2	2.9	3.9	1.6	0.8	11.7	13.1	1.5		0.8	1.8	
	533.0	6.8	8.8	2.1	2.2	4.5	9.0	1.7	9.8	3.0	1.0	10.6	9.1	2.1		0.9	1.5	
	536.6	9.8	7.5	2.4	2.3	4.1	7.3	2.9	4.9	1.7	0.6	9.9	12.8	1.5		0.4	1.3	
	583.0	7.3	6.6	2.2	2.1	3.8	7.0	2.4	5.0	2.0	0.8	10.9	11.1	1.5		0.9	1.6	

[a] Peaks for the corresponding naturally occurring isotopomer were observed.

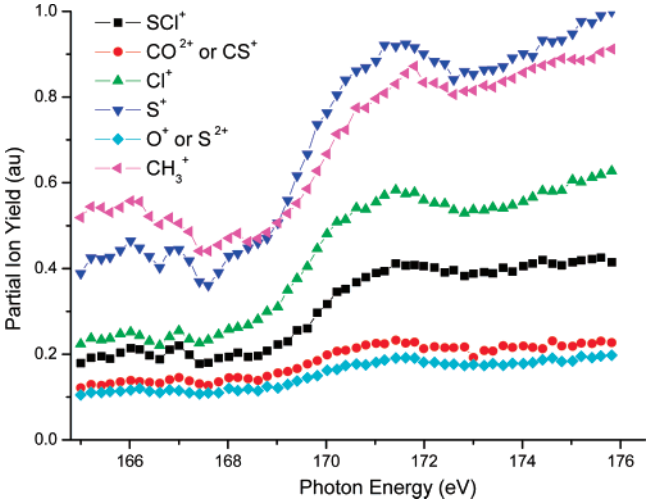

Figure 5. Partial Ion Yield spectrum for selected ions of $CH_3OC(O)SCl$ in the S 2p region.

transitions corresponding to transitions of the inner shell orbitals of the S $2p_{3/2}$ and S $2p_{1/2}$ to unspecified antibonding orbitals and/or Rydberg series. The close analysis of the ion production in this region could serve as a tool for the assignment of these features. With these facts in mind, more detailed partial ion yield (PIY) spectra have been obtained in the 165.0−175.0 eV range by recording the count rates of selected ions while the photon energy is scanned in steps of 0.2 eV (Figure 5). In these PIY spectra, each point corresponds to one time-of-flight spectrum measured at this defined photon energy. The intensity of each ionic fragment is obtained by fitting a Gaussian function to the time-of-flight spectra.

Although less resolved, the PIY spectra for the main single charged ions resemble the TIY spectrum of Figure 1. The production of ions increases as the photon energy increases, with a pronounced slope between 169.0 and 171.5 eV. The S^+ ion signal shows a steep enhancement at around the S 2p threshold. It becomes predominant up 169.0 eV (see Figure 5 and Table 1). Since multiple bond fissions are necessary to form this ion from the ionized $CH_3OC(O)SCl$, complex processes are expected to take place in the production of S^+. At the lowest energy examined, 165.0 eV (corresponding to the deep valence excitations), the contribution of this ion to the total ion production is also important, which could be a hint about the importance of non-resonant or direct double ionization processes in the internal energy redistribution before fragmentation. Other important contributing ions are CH_3^+ and Cl^+. Both ions can be formed by single bond ruptures of the CH_3-O and S−Cl single bonds, respectively. Thus, processes that involve excitations to the corresponding σ^*_{O-C} and σ^*_{S-Cl} antibonding orbitals, respectively, can be suggested. It is worth noting the parallelism of the TIY and the CH_3^+ ion signals below the ionization edge.

The heaviest fragment observed in the spectrum of Figure 5 is the SCl^+ ion. It should be noted that only a singly charged molecular ion can produce SCl^+ from ionized $CH_3OC(O)SCl$. In effect, even the whole remaining $CH_3OC{=}O$ group is lighter than SCl, and should be detected in the PEPICO spectra instead of SCl^+. Thus, the detection of this ion in the PEPICO spectra implies the following mechanism of dissociation:

$$CH_3OC(O)SCl^+ \rightarrow SCl^+ + \text{neutral products (nondetected)}$$

The simple rupture of the C−S bond could be understood as caused by electronic excitations from inner shell levels to the vacant σ^*_{C-S} orbital, which is know to play a relevant role in the electronic spectra of $CH_3C(O)SH$.[35] In connection with these remarks, it is relevant to note that the most important ion observed in the electron impact mass spectra at 70 eV, $CH_3OC{=}O^+$ ($m/z = 59$), has only a minor abundance at the energies examined in this work.[36]

Ionic Fragmentation Near the Cl 2p Shallow-Core Edge. The PEPICO spectra of $CH_3OC(O)SCl$ recorded at photon energies near the Cl 2p edge are shown in the Figure 6. The corresponding branching ratios are listed in Table 1. The S^+ and Cl^+ ions are now the most abundant fragments. The increment of the intensity of the H^+ ion at increasing incident photon energies even within the Cl 2p energy region can also be noticed (from 5% to 11%). Apart from a moderate enhancement of the Cl^+ ion signal, the PEPICO spectra in this region are very similar to those measured in the S 2p edge. New signals appear at $m/z = 17.5$ and 18.5 amu/q, corresponding to the double charged chlorine isotopes. The formation of doubly charged ions hints at least to the occurrence of triple ionization processes. Surprisingly, the molecular ion at $m/z = 126$ amu/q can still be observed at these energies as a low intensity but well-defined signal with the isotopomeric contribution at $m/z = 128$ amu/q.

Changes in the TOF spectral shape of the $m/z = 44$ peak can be noticed by going from the S 2p to the Cl 2p region. It is well-established that the analysis of ion peak shapes from a

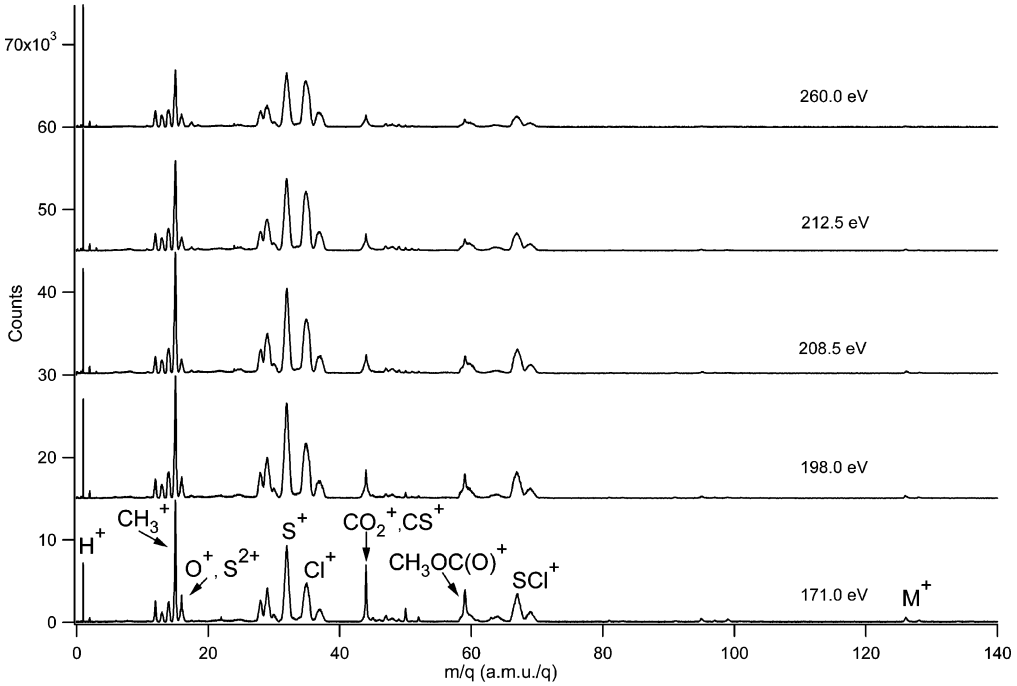

Figure 6. PEPICO spectra of $CH_3OC(O)SCl$ recorded near the Cl 2p edge.

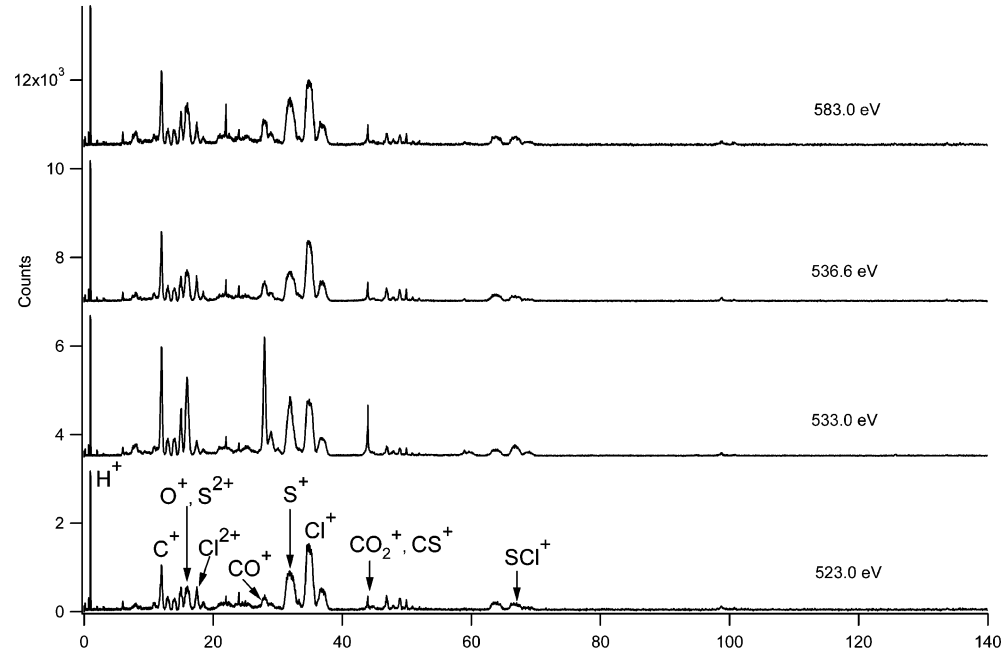

Figure 7. PEPICO spectra of $CH_3OC(O)SCl$ recorded near the O 1s edge.

PEPICO spectrum provides information concerning fragment ion kinetic energies. The production of two possible ions with the same value of mass/charge, CO_2^+ or CS^+ and different kinetic energy release, may be responsible for this observed change.

Ionic Fragmentation Near the O 1s Core Edge. PEPICO spectra of $CH_3OC(O)SCl$ have been recorded near the O 1s edge and are shown in Figure 7. In Table 1 the corresponding branching ratios are displayed for the main fragment ions. The intensity of the C^+ ion (5.2−8.8%) is always higher than the intensity of the methyl fragments $CH_x^+(x = 1, 2, 3)$. The most important ions near the O 1s edge are S^+, Cl^+, O^+ or S^{2+} and H^+. The intensity of the signal at 17.5 amuq, corresponding to the Cl^{2+} ion, is higher than that observed in the Cl 2p region. The molecular ion cannot be observed at these high energies.

A diminution in the $m/z = 29$ amu/q peak intensity, corresponding to the HCO^+ ion, can be observed. This fact can be correlated with the observed enhancement in the signal intensity of the ions H^+ and CO^+ in this energy region. Formyl cation was previously detected in the gas phase by mass spectrometric studies on the electron impact ionization of formaldehyde.[37] HCO^+ is believed to be an important intermediate in the chemistry of carbon monoxide in acidic environments. However, its observation in solution has been elusive for a long time.[38] Only recently was it possible to generate this species by the reaction of CO with the liquid superacid hydrofluoric acid-antimony pentafluoride ($HF-SbF_5$) under pressure.[39]

In this energy region, the main features in the spectra are dominated by atomic ions, while signals corresponding to ionic

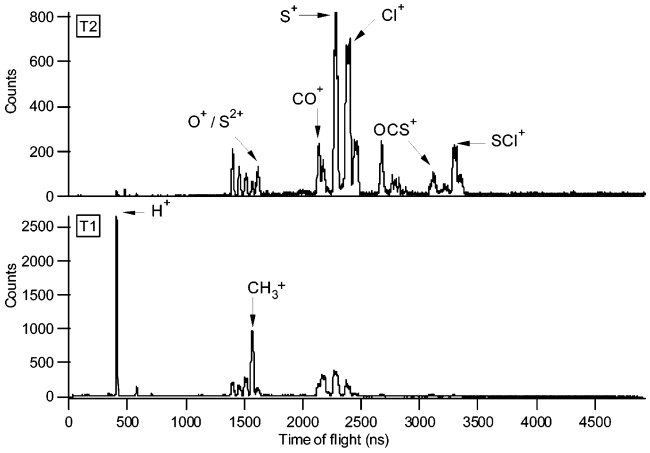

Figure 8. T1 and T2 projections of the PEPIPICO spectrum of $CH_3OC(O)SCl$ recorded at 212.5 eV on the S 2p resonance.

fragments such as $CH_3OC{=}O^+$ (59 amuq), OCS^+ (60 amu/q), and SCl^+ (67 amu/q) appear as low-intensity bands. Moreover, there is a remarkable diminution in the intensity of the signal at $m/z = 32$ amu/q together with an increment in the m/z 16 (S^{2+}) peak intensity. The Cl^+ ion signal is more intense than the S^+ ion, contrary to the observation in the other spectral regions. Thus, strong atomization processes occur at these high photon energies that include the formation of multiply charged molecular ions. An increase in the peak intensities corresponding to the ions H^+, C^+, O^+, or S^{2+}, together with the diminution in the intensity of the CH_3^+, HCO^+, H_2CO^+, S^+, CO_2^+, COS^+, SCl^+, and CH_3OCO^+ ion signals is observed by going from S 2p to the O 1s region. Near the O 1s edge, the signals at 6 and 8 amu/q can be assigned with confidence to the doubly charged ions C^{2+} and O^{2+}, respectively.

In particular, the TOF mass spectrum of $CH_3OC(O)SCl$ measured at the main transition below the 1s O ionization edge (533.0 eV) shows noticeable differences with the PEPICO spectra obtained in the other photon energy region near the 1s O edge. A clear increase in the intensity of the signals corresponding to the ions CO^+, O^+ or S^{2+} and C^+ results evident (Figure 7). It is noteworthy that all these fragments are related with the $-OC(O)S-$ central moiety. The O 1s $\rightarrow$ $\pi^*_{C=O}$ excitation may give raise to the Resonant Auger processes that further results in the ejection of valence electrons from molecular orbitals involving the O−C and C−S single bonds. Thus, the preferred production of these ions can be understood.

PEPIPICO Spectra. Two-dimensional PEPIPICO spectra for the correlation between one electron and two positive ions were recorded at several photon energies near the S 2p edge, Cl 2p edge and O1s edge. A multicoincidence measurement allows the identification of the various ions produced in the same photoionization event. The analysis of the PEPIPICO spectra is useful for identifying several two-, three- and four-body dissociation mechanisms which especially follow Auger decay mechanisms.[40,41]

Projections of PEPIPICO spectra of $CH_3OC(O)SCl$ on the T1 and T2 axes were obtained by integrating the signal intensities over the time domains. These projections for the spectrum recorded at the S 2p threshold are depicted in the Figure 8. The H^+ ion signal dominates the T1 domain followed in importance by the CH_x^+ ($x = 0, 1, 2, 3$) group of ions and those related to m/z values of 28, 29, 32, and 35 amu/q. The heaviest observed fragment in the T2 domain is SCl^+. The T2 projection is dominated by ion signal corresponding to the m/z ion ratio of 32 amuq, while other fragments with significant intensity are those related to m/z values of 16, 28, 29, 35, and 44 amu/q. The CH_x^+ ($x = 0, 1, 2$) group of ions also appear in the T2 domain, implying that CH_x^+ ($x = 1, 2, 3$) ions undergo further dissociation by losing one hydrogen atom to form the CH_{x-1}^+ ($x = 1, 2, 3$) species. The S^+, Cl^+, CO^+, and HCO^+ can be formed in different processes where they are both the lightest and the heaviest fragments. When comparing T1 and T2 PEPIPICO projection spectra of $CH_3OC(O)SCl$ recorded around the Cl 2p, S 2p, and O 1s energy regions, some differences are observed in the group of intensities of the CH_x^+ ($x = 0, 1, 2$) and O^+ or S^{2+} ions, denoting some minor changes in the fragmentation by varying the incident energy.

The PIPICO projections for the time difference (T2 minus T1) domain were also analyzed. Figure 9 shows the spectrum taken at 212.5 eV on the S 2p resonance with an assignment of the main peaks. The progression of coincidences involving the

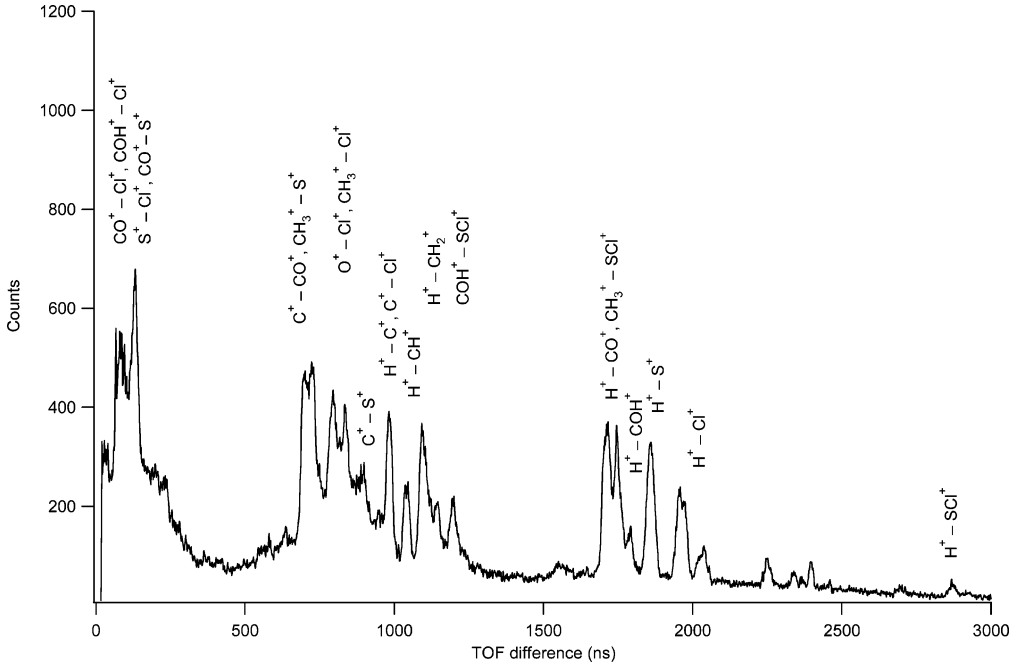

Figure 9. PIPICO projection spectrum of $CH_3OC(O)SCl$ recorded at 212.5 eV on the S 2p resonance.

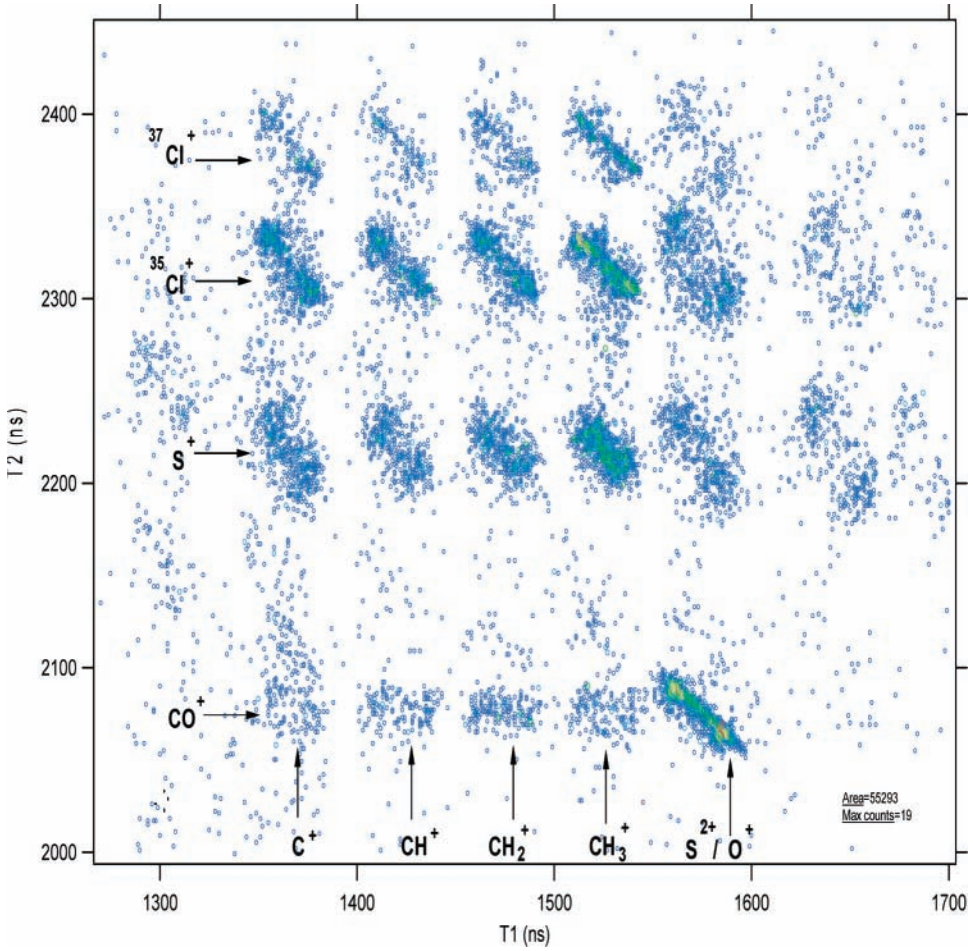

Figure 10. Enlargement of the PEPIPICO spectrum of $CH_3OC(O)SCl$ obtained at 533.0 eV photon energy in the ranges of *m*/*z* 12−16 and 28−37 amu/q in the T1 and T2 domains, respectively.

$H^+-CH_x^+$ ($x = 0, 1, 2$) series of ions is clearly observed. The Partial Double Coincidence Yields (PDCY) obtained from the PEPIPICO spectra for the islands involving the $H^+-CH_x^+$ ($x = 0, 1, 2$) series of ions were 4%, 3%, and 2%, respectively and no coincidence is observed for the $H^+-CH_3^+$ ions, as expected. The excitation of shallow- and inner-core electrons in $CH_3OC(O)SCl$ seems to proceed in such a way that the positive charge is mainly placed on the CH_x^+ ($x = 0, 1, 2$)$-H^+$ fragments:

$$CH_3OC(O)SCl^{2+} \rightarrow H^+ + CH_x^+ (x = 0, 1, 2) + \text{neutral fragments (not detected)}$$

The Partial Double Coincidence Yield (PDCY) for the island between ions with *m*/*z* values of 15 amu/q (CH_3^+) and 32 amu/q (S^+) showed the highest intensity (14%) in the S 2p region. An increase in the intensity of the island involving the H^+-C^+ ions is observed by going from S 2p (4%) to the O 1s region (12%). The PDCY for the island between the ions H^+ and Cl^+ in the O 1s is higher than that observed in the S 2p and Cl 2p regions.

Other competitive channels are observed, mainly involving atomic charged fragments. These coincidences are better defined in the original PEPIPICO spectra. Thus, as anticipated from the qualitative analysis of the projection spectra, in the case of a rather complex molecule such as $CH_3OC(O)SCl$, several islands are expected in the PEPIPICO spectra, and hence a complete interpretation of the spectra is not straightforward. Thus, in the analysis of the PEPIPICO spectra, the following two aspects were taken into account. First, due to the inherent limited resolution used in the experiments, for islands involving *m*/*z* values of 16 amu/q, the distinction between O^+ and S^{2+} ions is not always feasible. Second, peaks corresponding to double coincidences involving the *m*/*z* values of 1, 12, 16, 32, and 35 amu/q are the most intense reflecting the importance of the atomization processes in the dissociation mechanisms of $CH_3OC(O)SCl$. These processes may be originated by several multi-body dissociation events that conduce to the same final couple of atomic ions, making ambiguous the analysis of these coincidences. Taking into consideration these comments, in a first approximation, the attention is paid on selected pairs of ions, for which both a good statistics and well-defined shape are observed. Therefore, the double coincidences considered here are: O^+CO^+, CHx^+/Cl^+ ($x = 0, 1, 2, 3$), and S^+/Cl^+.

1. Coincidence between Ions with m/z Values of 28 amu/q (CO^+) and 16 amu/q (O^+). This coincidence is depicted on the Figure 10. The observed slope close to −1 can be explained by a deferred charge separation (DCS) four-body ion process:[41]

$$CH_3OC(O)SCl^{2+} \rightarrow CH_3OC(O)^{2+} + SCl$$

$$CH_3OC(O)^{2+} \rightarrow CH_3 + CO_2^{2+}$$

$$CO_2^{2+} \rightarrow O^+ + CO^+$$

It is quite unlikely that the *m*/*z* = 16 amu/q signal involves the S^{2+} ion, instead of the ion O^+, since the fragments should

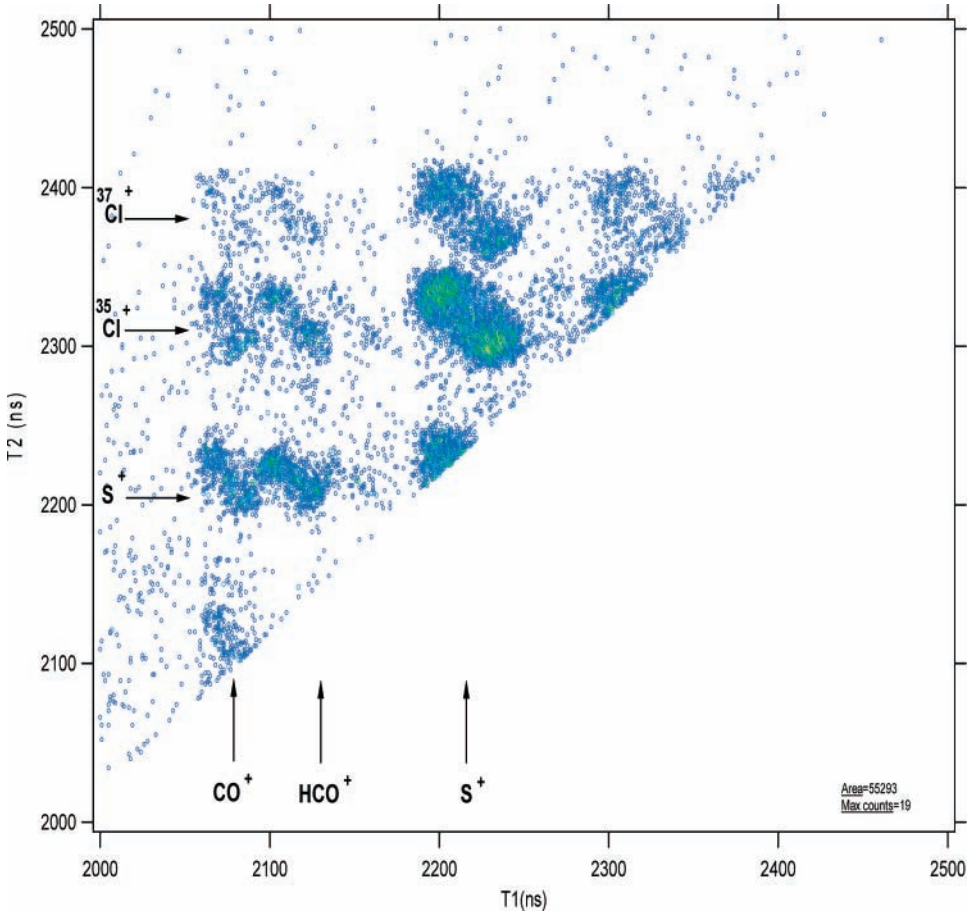

Figure 11. Enlargement of the PEPIPICO spectrum of $CH_3OC(O)SCl$ obtained at 533.0 eV photon energy in the ranges of *m*/*z* 28−32 and 32−37 amu/q in the T1 and T2 domains, respectively.

come at least from the triple charged molecular ion, $CH_3OC(O)SCl^{3+}$. It is also remarkable that the experimental slope for this coincidence can be also explained by a second type of four-body ion pair process DCS, in which the neutral methyl fragment is generated in the first place, while the SCl species is generated in a second step. In both cases the last step dissociation dynamics yield O^+ and CO^+ from double charged carbon dioxide. Masouka et al. have studied the dissociation of CO_2^{2+} by the coincidence PEPIPICO method.[42] A strong coincidence between O^+ and CO^+ ions was observed in the CO_2 spectra measured at 90 eV. The analysis of the kinetic energy release distribution observed for these ionic fragments suggests that the observed channels cannot be explained by a simple framework at low excitation energies whereby the doubly charged molecular ion is directly produced by a single photon absorption followed by the dissociation into two ionic fragments. Thus, the proposed mechanism to explain the coincidence between O^+ and CO^+ in the spectra of $CH_3OC(O)SCl$ must be taken to be tentative.

2. Coincidence between Ions with m/z Values of 32 amu/q (S^+) and 35 amu/q (Cl^+). The observed slope (Figure 11) of −0.93 for this coincidence can be explained by the following three-body dissociation process in a DCS scheme:

$$CH_3OC(O)SCl^{2+} \rightarrow CH_3OC(O) + SCl^{2+}$$

$$SCl^{2+} \rightarrow S^+ + Cl^+$$

3. Coincidence between Ions with m/z Values of 15 amu/q (CH_3^+) and 35 amu/q (Cl^+). The coincidence island for these two fragments is shown in Figure 10. The observed slope for the CH_3^+/Cl^+, that is approximately −1, can be explained by the following three-body ion pair process DCS:

$$CH_3OC(O)SCl^{2+} \rightarrow CH_3Cl^{2+} + NP$$

$$CH_3Cl^{2+} \rightarrow CH_3^+ + Cl^+$$

A four-body ion pair mechanism DCS can also be responsible for this island, in agreement with the following processes:

$$CH_3OC(O)SCl^{2+} \rightarrow CH_3SCl^{2+} + CO_2$$

$$CH_3SCl^{2+} \rightarrow S + CH_3Cl^{2+}$$

$$CH_3Cl^{2+} \rightarrow CH_3^+ + Cl^+$$

Coincidences between CH_x^+ ($x = 0, 1, 2$) and Cl^+ show slight changes in the slope when the hydrogen extrusion increases. Little differences are expected in the slope of double coincidences involving CH_x^+ ($x = 0, 1, 2$) when compared with CH_3^+ because of the low mass of the H^+ ion. This fact might evidence that the mechanisms involved in the formation of CH_x^+ ($x = 0, 1, 2$) ions can be sequential via the formation of CH_3^+ ion in the very first step. Thus, four-body ion pair processes need to be invoked to explain the coincidence between CH_2^+ and Cl^+ ions.

Conclusions

The TIY spectra of shallow-core levels S 2p and Cl 2p and inner-shell level O 1s of $CH_3OC(O)SCl$ were obtained in the

range 100−1000 eV by using synchrotron radiation and coincidence detection techniques. Complex electronic processes occur at resonant energies below the S 2p ionization edge, which appear to be characteristic for −SC(O)− containing compounds. The observed features in the TIY spectra could be related with several phenomena such as electronic transitions to vacant orbitals with contributions of spin−orbit splitting of the S 2p terms of the ionized species, autoinization of transitions to Rydberg levels or a contribution of both of them. Thus, this family of compounds deserves further studies involving the use of electron spectroscopy based methods to cover these aspects.

The analysis of the PEPICO spectra reveals a preferential production of S^+ ions in the S 2p absorption edge that would seem to be an evidence for state-specific fragmentations. Electronic excitations from inner shell levels to vacant σ^*_{C-S} and/or σ^*_{S-Cl} orbitals in $CH_3OC(O)SCl$ could be responsible for this specificity. The σ^*_{C-S} antibonding orbital is know to play a relevant role in the electronic spectra of related molecules.[35] For the triatomic species OCS and CS_2, the ion yield spectra near the L and K absorption edges show definite transitions to the σ^* orbitals.[43−46] Moreover, a slightly state-specific photofragmentation of carbonyl sulfide following sulfur 1s excitation has been observed as indicated by an atomic ion increment at the onset of the S 1s excitation. The cleavage of the carbon−sulfur bond is favored over the cleavage of the oxygen−carbon bond both above and below the sulfur 1s ionization threshold.[47]

From PEPICO and PEPIPICO spectra possible dissociation mechanisms involved in the fragmentation of the $CH_3OC(O)SCl$ followed the electronic ionization have been deduced. Two- and three-body processes, the later via a secondary decay sequential dissociation mechanism, have been proposed. Coincidences concerning the series of CH_x^+ ions ($x = 0, 1, 2$) arise from four body dissociation mechanisms by the loss of hydrogen atoms from the CH_3^+ ion.

Acknowledgment. This work has been largely supported by the Brazilian Synchrotron Light Source (LNLS) under proposals D05A-TGM-906 and D08A-SGM-907. The authors thank the "Programa de ayuda financiera para investigadores de instituciones latinoamericanas y del caribe" (LNLS). The authors wish to thank Arnaldo Naves de Brito and his research group for fruitful discussions and generous collaboration during their several stays in Campinas and the SGM and TGM beamline staffs for their assistance throughout the experiments. They are indebted to the Agencia Nacional de Promoción Científica y Tecnológica (ANPCyT), Consejo Nacional de Investigaciones Científicas y Técnicas (CONICET), and the Comisión de Investigaciones Científicas de la Provincia de Buenos Aires (CIC), República Argentina, for financial support. They also thank the Facultad de Ciencias Exactas, Universidad Nacional de La Plata, República Argentina for financial support. R.M.R. also thanks the Fundación Antorchas for a grant. CODV especially acknowledges the DAAD, which generously sponsors the DAAD Regional Program of Chemistry for the República Argentina supporting Latin-American students to make their PhD in La Plata.

References and Notes

(1) Ueda, K.; Eland, J. H. D. *J. Phys. B: At. Mol. Opt. Phys.* **2005**, *38*, S839.

(2) Continetti, R. E. *Annu. Rev. Phys. Chem.* **2001**, *52*, 165.

(3) Hsieh, S.; Eland, J. H. D. *J. Phys. B: At. Mol. Opt. Phys.* **1997**, *30*, 4515.

(4) Eberhardt, W.; Sham, T. K.; Carr, R.; Krummacher, S.; Strongin, M.; Weng, S. L.; Wesner, D. *Phys. Rev. Lett.* **1983**, *50*, 1038.

(5) Erman, P.; Karawajczyk, A.; Rachlew, E.; Stankiewicz, M.; Yoshiki Franzen, K. *J. Chem. Phys.* **1997**, *107*, 10827.

(6) Hanson, D. M. *Adv. Chem. Phys.* **1990**, *77*, 1.

(7) Mueller-Dethlefs, K.; Sander, M.; Chewter, L. A.; Schlag, E. W. *J. Phys. Chem.* **1984**, *88*, 6098.

(8) Boo, B. H.; Saito, N. *J. Electron Spectrosc. Relat. Phenom.* **2003**, *128*, 119.

(9) Miron, C.; Simon, M.; Leclercq, N.; Hansen, D. L.; Morin, P. *Phys. Rev. Lett.* **1998**, *81*, 4104.

(10) Nagaoka, S.-i.; Fujibuchi, T.; Ohshita, J.; Ishikawa, M.; Koyano, I. *Int. J. Mass Spectrom. Ion. Process.* **1997**, *171*, 95.

(11) Baba, Y. *Low Temp. Phys.* **2003**, *29*, 228.

(12) Erben, M. F.; Romano, R. M.; Della Védova, C. O. *J. Phys. Chem. A* **2004**, *108*, 3938.

(13) Erben, M. F.; Romano, R. M.; Della Védova, C. O. *J. Phys. Chem. A* **2005**, *109*, 304.

(14) Erben, M. F.; Della Védova, C. O. *Inorg. Chem.* **2002**, *41*, 3740.

(15) Erben, M. F.; Della Védova, C. O. *Helv. Chim. Acta* **2003**, *86*, 2379.

(16) Erben, M. F.; Geronés, M.; Romano, R. M.; Della Védova, C. O. *J. Phys. Chem. A* **2006**, *110*, 875.

(17) Erben, M. F.; Della Védova, C. O.; Romano, R. M.; Boese, R.; Oberhammer, H.; Willner, H.; Sala, O. *Inorg. Chem.* **2002**, *41*, 1064.

(18) Manke, G. C., II; Setser, D. W. *J. Phys. Chem. A* **2000**, *104*, 11013.

(19) Lira, A. C.; Rodrigues, A. R. D.; Rosa, A.; Gonçalves da Silva, C. E. T.; Pardine, C.; Scorzato, C.; Wisnivesky, D.; Rafael, F.; Franco, G. S.; Tosin, G.; Lin, L.; Jahnel, L.; Ferreira, M. J.; Tavares, P. F.; Farias, R. H. A.; Neuenschwander, R. T. In *First Year Operation of the Brazilian Sinchrotron Light Source*, European Particle Accelerator Conference, Stockholm, 1998; EPAC.

(20) de Fonseca, P. T.; Pacheco, J. G.; Samogin, E.; de Castro, A. R. B. *Rev. Sci. Instr.* **1992**, *63*, 1256.

(21) Frasinski, L. J.; Stankiewicz, M.; Randall, K. J.; Hatherly, P. A.; Codling, K. *J. Phys. B: At. Mol. Phys* **1986**, *19*, L819.

(22) Eland, J. H. D.; Wort, F. S.; Royds, R. N. *J. Electron Spectrosc. Relat. Phenom.* **1986**, *41*, 297.

(23) Naves de Brito, A.; Feifel, R.; Mocellin, A.; Machado, A. B.; Sundin, S.; Hjelte, I.; Sorensen, S. L.; Bjorneholm, O. *Chem. Phys. Lett.* **1999**, *309*, 377.

(24) Jolly, W. L.; Hendrickson, D. N. *J. Am. Chem. Soc* **1970**, *92*, 1863.

(25) Adams, D. B. *J. Electron Spectrosc. Relat. Phenom.* **1993**, *61*, 241.

(26) Thomas, T. D.; Saethre, L. J.; Sorensen, S. L.; Svensson, S. *J. Chem. Phys.* **1998**, *109*, 1041.

(27) Magnuson, M.; Guo, J.; Såthe, C.; Rubensson, J.-E.; Nordgren, J. *Phys. Rev. A* **1999**, *59*, 4281.

(28) Situmeang, R.; Thomas, D. T. *J. Electron Spectrosc. Relat. Phenom.* 1999, *98*−*99*, 105.

(29) Bozek, J. D.; Carroll, T. X.; Hahne, J.; Sæthre, L. J.; True, J.; Thomas, T. D. *Phys. Rev. A* **1998**, *57*, 157.

(30) Borve, K. J.; Saethre, L. J.; Svensson, S. *Chem. Phys. Lett.* **1999**, *310*, 439.

(31) Cheng, B.-M.; Chew, E. P.; Liu, C.-P.; Yu, J.-S. K.; Yu, C.-h. *J. Chem. Phys.* **1999**, *110*, 4757.

(32) Frisch, M. J.; Trucks, G. W.; Schlegel, H. B.; Scuseria, G. E.; Robb, M. A.; Cheeseman, J. R.; Zakrzewski, V. G.; Montgomery, J. A.; Stratman, R. E.; Burant, J. C.; Dapprich, S.; Millam, J. M.; Daniels, A. D.; Kudin, K. N.; Strain, M. C.; Farkas, O.; Tomasi, J.; Barone, V.; Cossi, M.; Cammi, R.; Menucci, B.; Pomelli, C.; Adamo, C.; Clifford, S.; Ochterski, J.; Petersson, G. A.; Ayala, P. Y.; Cui, Q.; Morokuma, K.; Malick, D. K.; Rabuck, A. D.; Raghavachari, K.; Foresman, J. B.; Cioslovski, J.; Ortiz, J. V.; Stefanov, B. B.; Liu, G.; Liashenko, A.; Piskorz, P.; Komaromi, I.; Gomperts, R.; Martin, R. L.; Fox, D. J.; Keith, T.; Al-Laham, M. A.; Peng, C. Y.; Nanayakkara, A.; Gonzales, C.; Challacombe, M.; Gill, P. M. W.; Johnson, B.; Chen, W.; Wong, M. W.; Andres, J. L.; Gonzales, C.; Head-Gordon, M.; Replogle; Pople, J. A. *Gaussian 98*, Revision A.7 ed.; Gaussian: Pittsburgh, PA, 1998.

(33) Nenner, I.; Beswick, J. A. Molecular Photodissociation and Photoionization. In *Handbook on Synchrotron Radiation*; Marr, G. V., Ed.; Elsevier Science Publishers: Amsterdam, 1987; Vol. 2, pp 355−462.

(34) Svensson, S.; Naves de Brito, A.; Keane, M. P.; Correia, N.; Karlsson, L. *Phys. Rev. A* **1991**, *43*, 6441.

(35) Nagata, S.; Yamabe, T.; Fukui, K. *J. Phys. Chem.* **1975**, *79*, 2335.

(36) Stein, S. E. *Mass Spectra*; NIST Standard Reference Database Number 69; National Institute of Standards and Technology: Gaithersburg, MD, 2003 (http://webbook.nist.gov).

(37) Reed, R. I. *Trans. Faraday Soc.* **1956**, *52*, 1195.

(38) Olah, G. A.; Dunne, K.; Mo, Y. K.; Szilagyi, P. *J. Am. Chem. Soc.* **1972**, *94*, 4200.

(39) de Rege, P. J. F.; Gladysz, J. A.; Horváth, I. T. *Science* **1997**, *276*, 776.

(40) Eland, J. H. D. *Mol. Phys.* **1987**, *61*, 725.
(41) Simon, M.; Lebrun, T.; Martins, R.; de Souza, G. G. B.; Nenner, I.; Lavollee, M.; Morin, P. *J. Phys. Chem.* **1993**, *97*, 5228.
(42) Masuoka, T.; Nakamura, E.; Hiraya, A. *J. Chem. Phys.* **1996**, *104*, 6200.
(43) Esser, B.; Ankerhold, U.; Anders, N.; von Busch, F. *J. Phys. B: At. Mol. Opt. Phys.* **1997**, *30*, 1191.
(44) Perera, R. C. C.; LaVilla, R. E. *J. Chem. Phys.* **1984**, *81*, 3375.
(45) Feng, R.; Cooper, G.; Sakai, Y.; Brion, C. E. *Chem. Phys.* **2000**, *255*, 353.
(46) Karawajczyk, A.; Erman, P.; Hatherly, P.; Rachlew, E.; Stankiewicz, M.; Yoshiki Franzén, K. Phys. Rev. A **1998**, *58*, 314.
(47) Neville, J. J.; Tyliszczak, T.; Hitchcock, A. P. *J. Electron Spectrosc. Relat. Phenom.* **1999**, *101*−*103*, 119.